Sediment transport modelling (TELEMAC-3D + GAIA) case study: sand disposals in the Western Scheldt

T. Wolf, W.A. Breugem, K. Chu, B. Decrop,
G. Van Holland
International Marine and Dredging Consultants n.v.
Van Immerseelstraat 66, 2018 Antwerp, Belgium
thom.wolf@imdc.be

Y. Plancke, J. Stark
Flanders Hydraulics Research – Antwerp, Belgium
Berchemlei 115, 2140 Antwerpen

Abstract—**In this study, the three-dimensional coupled (TELEMAC-3D + GAIA) morphodynamic Scheldt model is used to investigate the behaviour of sand disposals in the Western Scheldt by simulating the experimental disposal campaign of 2019 at the Put van Hansweert. A validation of the hydrodynamics shows that the Scheldt model is able to reproduce accurately water level predictions throughout the Scheldt estuary and good two/three-dimensional velocity patterns near the Put van Hansweert. By performing a Brier Skill Score analysis, it is shown that the simulated morpho-dynamics at the project site has the performance indication 'Good'. This reveals that the Scheldt model is suited for scenario analysis.**

By using the end state of a disposed sediment cloud from a multi-phase CFD simulation, realistic initial conditions of the sediment concentration are implemented by means of a horizontal & vertical interpolation on the TELEMAC-3D mesh. The results show that in the first five weeks during the disposals, 40% of disposed sediment is not encountered at the disposal local, which is in agreement with the measured loss rates. Most of the 0.9 [M m³] disposed sediment tends to migrate in an upstream direction. By performing multiple sensitivity analyses, it is found that the stability of the disposed sediment is mostly affected by the choice of the equilibrium near-bed concentration formula and by the choice of the number and distribution of the vertical nodes in TELEMAC-3D.

I. INTRODUCTION

Maintenance of the navigation channel(s) in the Western Scheldt and Sea Scheldt is necessary in order to preserve the navigability for passing vessels. This maintenance encompasses the dredging of sand and other fine materials, as well as the disposal of these materials in strategically chosen areas in the Western Scheldt. These disposal areas are currently situated on shoals or in (side-) channels (Figure 1). A proposition to shift the disposal of sediment from these areas to deeper parts (pits) of the Western Scheldt exists, however the behaviour of the disposed sediment in these deeper parts is not fully understood.

Based on gathered bathymetric data during experimental disposal campaigns, volume evolutions have been analysed ([1]; [2]). Yet, the spreading and erosive behaviour of the disposed sediment in the deep pits on timescales of days to months remains unclear.

To answer these questions, several numerical models have been implemented [3]. These modelling studies showed that two-dimensional models show limitations to predict the transport of deposited sediment from the pits and showed the need for future studies using three-dimensional sediment transport models. The advantage of a three-dimensional model is that secondary circulations are resolved and hence, they do not need to be parametrized. This is particularly important, given the effect of the salinity on the secondary circulation in the study area, as these effects are not included in typical two-dimensional helicoidal flow parametrizations.

Therefore, in this study, a three-dimensional morphodynamical model is utilized to investigate the behaviour of the disposed sand in a hindcast of the experimental disposal campaign of 2019 at the Put van Hansweert ([2]; [4]).

The TELEMAC-3D module (version 8.1) is applied for the hydrodynamical calculations which solves the three-dimensional shallow water equations (with or without the hydrostatic pressure hypothesis) and the transport equations of intrinsic quantities (temperature, salinity, suspended sediment concentration). The sediment transport and morpho-dynamics are simulated using GAIA (version 8.1), which is the latest sediment transport code of the TELEMAC modelling suite.

II. HYDRODYNAMIC MODEL SETUP

The grid of the Scheldt model consists of unstructured triangular elements. Parts of the computational mesh and bathymetry of the Scheldt model are based on the SCALDIS model, which has been developed at Flanders Hydraulics Research [5]. The Scheldt model contains 214,416 calculation points in the two-dimensional grid and 397,889 elements. Twelve points are used for the vertical discretization. This leads to 2,572,992 calculation points for the entire three-dimensional model. These 12 vertical layers are located at 0%, 1%, 3%, 5%, 10%, 17%, 21%, 44%, 58%, 71%, 85% and 100% of the water depth. The high resolution near the bottom ensures that the model resolves the large sediment concentration gradient in the suspended sediment transport. The horizontal resolution (length of the sides of the
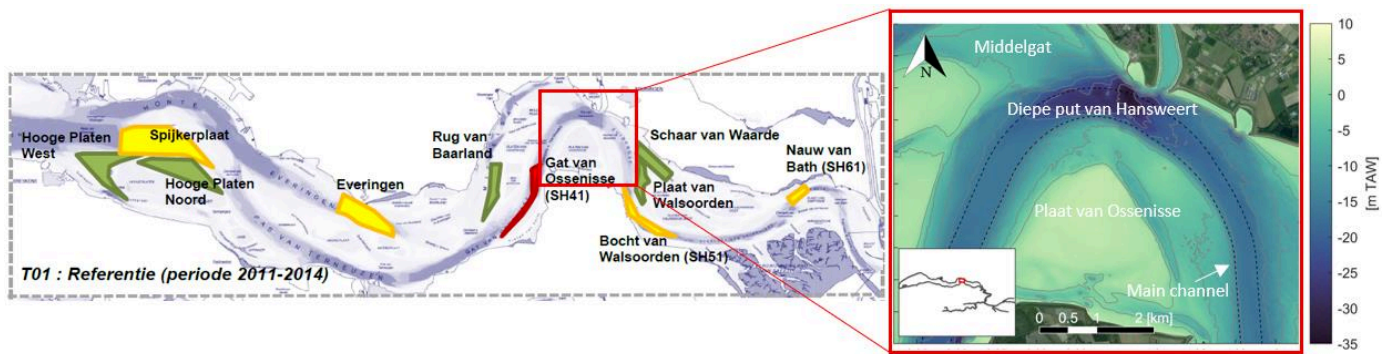
Figure 1 Left: Dumping strategy for the Western Scheldt (historical strategy for the period 2011-2014; colours indicate the intensity of the deposits; green to red = from low to high intensity).Source: [1]. Right: Zoomed-in red box with bathymetry of the Put van Hansweert disposal area.

triangular elements) varies between 3.6 [m] (mainly at Upper Sea Scheldt) and 400 m (Figure 2). In the coastal strip the resolution varies between 200 [m] and 400 [m] depending on the depth. The resolution in the Western Scheldt is approximately 120 [m], with refinements near the project area at the Put van Hansweert of up to 15 [m].
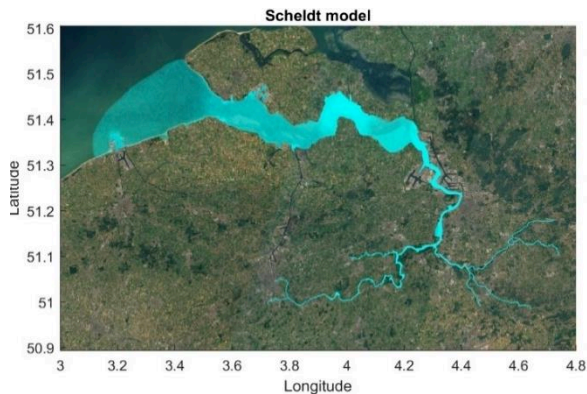

Figure 2 The computational mesh of the Scheldt model.

The model contains an open downstream boundary at the sea mouth of the Western Scheldt and eight upstream boundaries. Time series of water levels, velocities and salinity are imposed on the downstream open boundary. The time series of water levels and velocities come from the large-scale in-house developed iCSM model [6]. This model simulates tidal and wind-driven currents in the North Sea and other parts of the continental shelf. It is forced by hydrodynamic data from the OSU/TPXO model [7] for astronomical tidal components and by meteorological data (wind velocity and air pressure) obtained from the ERA-5 meteorological model. From the iCSM model, results of water levels and depth-average velocities are interpolated on the open downstream sea boundary of the Scheldt model via an in-house boundary nesting tool. The downstream precondition for salinity is based on either average representative values or measured values at the Vlakte van de Raan. There are eight upstream boundaries where flow rates and salinity are imposed.

Initial conditions of the model consist of spatially varying conditions for water levels and three-dimensional fields of velocity and salinity. These conditions are determined on the basis of a spin-up calculation of one day. An initial field has

been created for the salinity from measured salinity data using horizontal interpolation.

The model is being used to simulate periods ranging from one day to two months. The following model settings have been used in the simulations of hydrodynamics and the salinity (Table 1).

TABLE 1 MODEL PARAMETERS SETTINGS OF THE SCHELDT MODEL

Parameter	Value
Time step	10 [s]
Initial conditions	Spin-up conditions for water levels, currents and interpolated salinity field
Number of vertical nodes	12 (three-dimensional model)
Version TELEMAC	TELEMAC-3D (goblinshark branch based on version 8.1)
Salt transport	On
Wind	Off
Roughness formula	Nikuradse
Bed roughness value	Spatially varying roughness field
Vertical turbulence model	6: GOTM (using K-epsilon model with second order closure for the buoyancy flux)
Horizontal turbulence model	4: Smagorinski
Scheme for advection of velocities	1: characteristic method
Scheme for advection of tracers	13: Leo Postma for tidal flats
Solver	7: GMRES

III.   HYDRODYNAMIC VALIDATION

The RMSE value of water levels for the period of May-June 2017 is presented in Figure 3. It can be noted that, at the downstream part of the model (station Bol van Heist) the error is equal to 0.08 [m] and remains below 0.14 [m] along the estuary until Antwerp, which is the area of interest of the present paper. Near the Put van Hansweert at the measurement station of Hansweert, the error is 0.10 [m]. This is considered to be a good model performance.
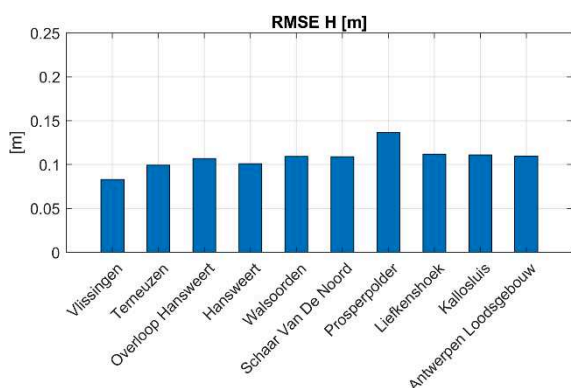
Figure3 RMSE [m] of the water level obtained for the various measuring points along the estuary, for the period 15/05/2017 - 02/06/2017

By using the model qualification based on the RMAE (relative mean absolute error) statistical parameter [8], which includes the accuracy of both the velocity magnitude and direction, comparisons between observed (with ADCP) and simulated depth-averaged velocities can be quantified. The RMAE statistics between simulated and measured velocities were calculated for the thirteen ADCP-campaigns near the project site. Values of the model qualification based on RMAE are provided in Figure 4. Thirteen available transects were used for the comparison and all, except for the 'Ossenisse_Dwarsraai -_20080407_Spring' transect, show a RMAE with the qualification 'Good' or 'Excellent'. Both the calculated RMSE and RMAE values of the five ADCP transect comparisons at the Diepe put van Hansweert are shown in Table 2.

Model qualification		RMAE [-]
Excellent		<0.2
Good		0.2-0.4
Reasonable/fair		0.4-0.7
Poor		0.7-1.0
Bad		>1.0
Not Applicable		-

Figure 4 Model qualification based on RMAE [8].

TABLE 2 COMPARISON OF RMSE AND RMAE OF VELOCITIES ALONG THE SELECTION OF ADCP TRANSECTS AT DIEPE PUT VAN HANSWEERT.

Campaign	RMSE [cm/s]	RMAE[-]
Diepe_Put_Hansweert_20170720	17.4	0.18
Diepe_Put_Hansweert_20181214_Dwarsraai	15.0	0.21
Diepe_Put_Hansweert_20181214_Langsraaien	18.0	0.26
Diepe_Put_Hansweert_20181220_Dwarsraai	13.0	0.15
Diepe_Put_Hansweert_20181220_Langsraaien	11.8	0.17

Figure 5 shows the comparison between simulated and measured vertical velocity profiles at the middle of the ADCP-transect during the rising of the tide. Both the shape of the velocity profile and its magnitude are well represented in the model.
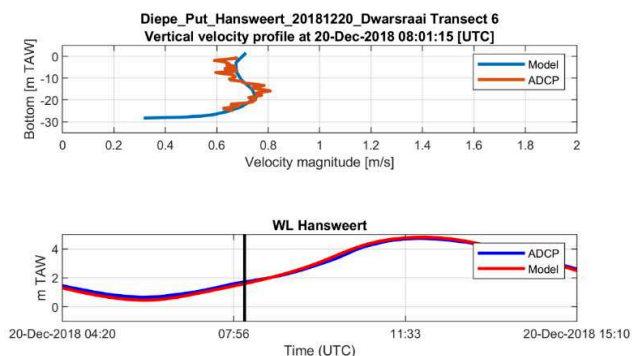

Figure 5 Top: Comparison of vertical velocity profiles between measurement velocities (ADCP campaign 20-Dec-2018 06:54:29, Diepe put van Hansweert) and simulated velocities. Bottom: Comparison of measured and simulated water level at Hansweert. The black line indicates the moment of comparison in the tide.

The three-dimensional behaviour of the simulated flow is further validated by comparing multiple times instances with measured ADCP-velocities taken during two ADCP-campaigns of December 2018 at the Put van Hansweert. An example is shown in (Figure 6). It shows that the overall patterns of the simulated transversal velocity components are in agreement with the measured ADCP transversal velocities. During the rise of the tide after slack water, both the simulated and measured transversal flows are at the bottom directed towards the outer bend and at the surface towards the inner bend.

A comparison of timeseries of the measured and modelled salinity near the water surface, just downstream and upstream of the Put van Hansweert, shows that the simulated salinity amplitude at the Overloop van Hansweert is underestimated by approximately 1 [psu]. Upstream of the Put van Hansweert at Baalhoek, both the amplitude and temporal variation of the salinity are well represented. A more quantitative analysis using statistical parameters (Table 3) shows that along a significant part of the Scheldt estuary, the salinity patterns are simulated well and that maximum RMSE reaches merely 0.93 [psu].

TABLE 3 STATISTICAL ANALYSIS BETWEEN SIMULATED AND MEASURED SALINITY VALUES (PERIOD 15/05/2017 - 02/06/2017) ALONG STATIONS IN THE SCHELDT ESTUARY.

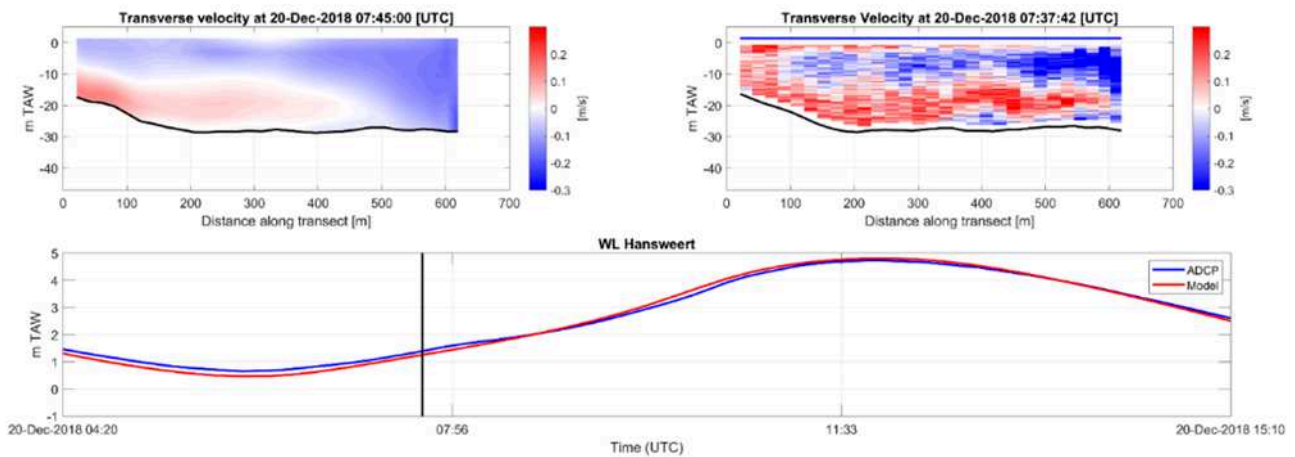| Nr	Station	Correlation coefficient R [-]	RMSE [psu]	Bias [psu]
1	Overloop Hansweert	0.91	0.51	-0.11
2	Baalhoek	0.96	0.93	0.82
3	Prosperpolder	0.93	0.46	0.01
4	Liefkenshoek	0.93	0.67	0.50
5	Oosterweel	0.97	0.91	0.65
6	Hemiksem	0.98	0.54	0.44

Figure 6 Comparison between simulated transverse flow velocity along transect in the 'Put van Hansweert' (top left) and measured transverse flow velocity (ADCP) along transect (top right). Red colour (positive velocity to the right (outer bend)), blue colour (negative velocity to the left (inner bend)). The bottom figure shows the measured (blue) and simulated (red) water level, the black vertical line indicates the moment of the ADCP-measurement

IV.   HYDRODYNAMIC RESULTS

For the investigation of the spatial distribution of the secondary circulation patterns near the Put van Hansweert, multiple transects along the thalweg with mean transversal velocities for spring tidal conditions are displayed in Figure 7. It shows that the upslope bottom velocities are present along a large part of the inner bend of the channel of Hansweert. The most pronounced circulation patterns are observed at the sharp bend of the Put van Hansweert transect 9. Furthermore, it is observed that transects 11 till 13 do not show similar tide averaged flow patterns as the upstream transects. This is likely due to the influence of the tidal flow coming from and going towards the side-branch of the

Middelgat (location indicated in Figure 7 and right subfigure of Figure 1).

The effect of lateral flow is substantially influenced by the density gradient due to the presence of salinity. This can be demonstrated by performing a run without salinity. When the effect of salinity is not included in the simulation, the simulated transversal velocity pattern changes significantly, and shows at patter that does not correspond to the ADCP transversal velocity (not shown). The tidally averaged transversal velocities along cross-sections in the channel near Hansweert show that multiple circulation cells are no longer present. Especially near the Put van Hansweert, the flow behaves as a typical helicoidal flow with a transversal surface
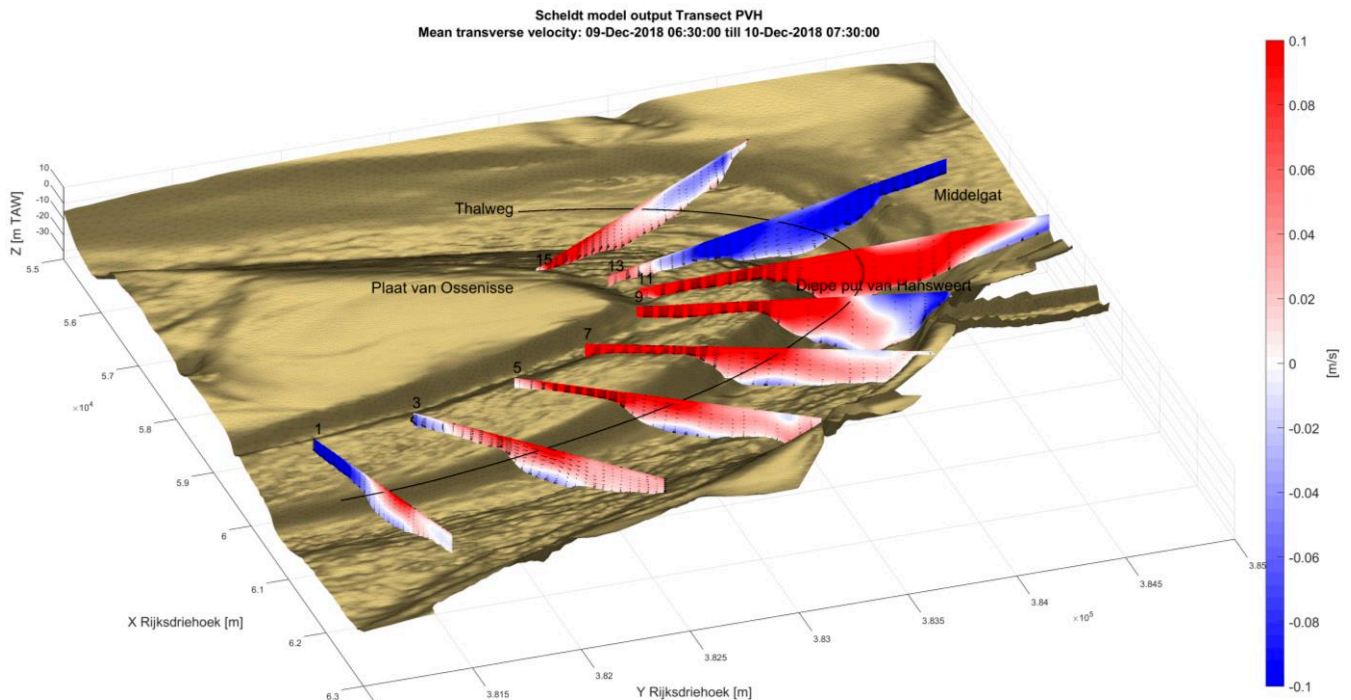

Figure 7 Simulated mean transverse flow velocities (for spring tidal conditions) at multiple transect perpendicular to the thalweg near the 'Put van Hansweert'. Red colour (positive velocity to the outer bend), blue colour (negative velocity to the inner bend).

flow directed towards the outer bend and a bottom flow directed towards the inner bend. This shows that the presence of salinity is vital to correctly simulate the complex local flow pattern and that it therefore should be included in the morpho-dynamic calculations.

V. MORPHODYNAMIC MODEL SETUP

A. GAIA settings

The used physical and numerical settings when coupling TELEMAC-3D to the sediment transport module GAIA are provided in Table 4. The sediment transport model is utilized to simulate two different sand fractions, hereafter called fraction1 and fraction2. Fraction1 is the disposed fraction with a d_{50} of 170 [μm] based on the analysis of barge samples performed by [4], which [9] applied as well in their study.

Fraction2 is the background sediment which is naturally present in the model through the definition of an initial layer thickness and has an attributed d_{50} of 220 [μm]. The choice of the natural sediment grain size is based on a grain size map shown from [10], where the d_{50} ranges between 200 - 250 [μm]. Furthermore, sediment samples [4] show that coarser sediments (d_{50} = 250 [μm]) are to be found downstream of the project site at the Overloop van Hansweert and finer sediments (d_{50} = 170 [μm]) upstream at the Drempel van Hansweert. A value in between this range is therefore representative to be used as d_{50} for the project site.

TABLE 4 MORPHOLOGICAL SETTINGS GAIA MODULE

Parameter (keywords GAIA)	Value
Finite volumes	YES
Minimal value of the water height	0.5 [m]
Number of sediment fractions	2
Classes sediment diameters	170; 220 [μm]
Classes initial fraction	0.0; 1.0
Bed-load transport formula for all sands	7 Van Rijn 1984)
Suspension transport formula for all sands	3 (Van Rijn 1984)
Hindered settling	YES
Hindered settling formula	1 (Whitehouse 2000; the equation is adapted for sand)
Skin friction correction	1
Formula for slope effect	1 (Koch and Flokstra, default β=1.3)
Formula for deviation	1 (Koch and Flokstra)
Sediment slide	NO
Layers non cohesive bed porosity	0.4 (default)
Active layer thickness	0.01 [m]
Number of layers for initial stratification	3
Layers initial thickness	1.E-6; x; x [m] (latter two spatially varying, in user_bed_init.f)

As initial layer thickness of the natural background sediment (fraction2 in GAIA) in the Western Scheldt, a spatially varying layer thickness has been applied in the Fortran function 'user_bed_init.f'. The height of the sediment layer is based on a combination of an existing TNO dataset [11] and the knowledge of the known locations of hard structures in the Western Scheldt [12].

B. Sediment sources

Initial conditions of the disposed sediment (fraction1 in GAIA) originate from multi-phase CFD simulations [13]. In these simulations a realistic amount of sediment, corresponding to a hopper volume of 4000 [m³], was disposed at the Put van Hansweert under flood flow conditions. The CFD model simulates 380 seconds, after which sediment concentration of the generated sediment plume (Figure 8) is extracted and horizontally & vertically interpolated on top of the TELEMAC-3D mesh.
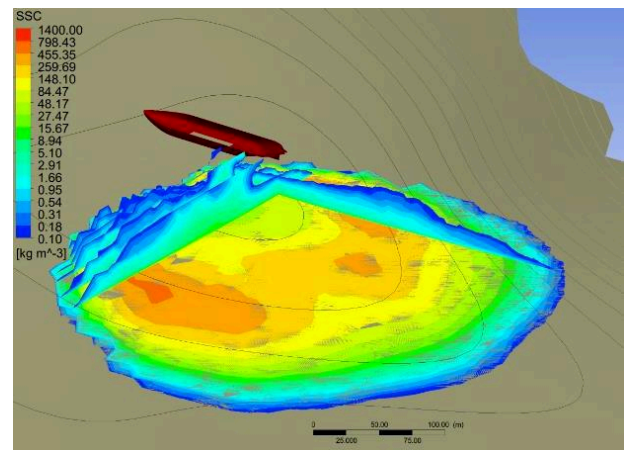

Figure 8 Contour plot of the suspended sediment concentration [kg/m³] from the CFD simulation scenario [13] at time instant t=380 s (end of the simulation). Black contour lines show the local bathymetry.

The disposal campaign of autumn 2019 has been reconstructed with the morpho-dynamic Scheldt model to investigate the disposed sediment loss over 2.5 months' time. The start of the simulation period is in accordance with the hydrodynamic starting period of May 2017. The disposed sediment volumes and disposal times are used from the recorded dredging data from the Flemish Ministry of Public works. The TELEMAC code was modified, such that the disposed volume was added to the suspended sediment in the model at the moment of each disposal where the amount of sediment from the CFD run is adjusted to match the volumes of the recorded disposal data. To take the flow direction into account on the disposal processes, the sediment plume is mirrored along the flow direction in case of ebb tide.

During the disposal campaign of 2019, two different sites were used in the Put van Hansweert for disposal. These are the outer bend (solid green bins 155 & 156 in Figure 9, hereafter called Northern disposal location) and the inner bend (solid yellow bins 292, 293 & 326 in Figure 9, hereafter called Southern disposal location). At the Northern disposal site, a total of 300,000 [m³] of sediment is disposed within the first three weeks of the simulation period and at the

Southern disposal site, a total of 700000 [m³] is disposed within the first eight weeks of the simulation period.

Measured bathymetric datasets from multibeam-echosounder campaigns reveal that the location of the disposal inside the bend of the Put van Hansweert is of key importance (Figure 9). The donut shape of the disposed sediment at the northern outer bend (bins 155 and 156) seems to be relatively stable, whereas at the same time, it is clearly visible that bedforms are actively migrating along the inner bend. From the small bed evolution in bins 223 till 225 it seems that there is a distinct border between these two regions. Approximately two months after the start of the disposal campaign, the disposed sediment is still visible in its confined spot in the deep part of the Put van Hansweert and maintains its donut shape.
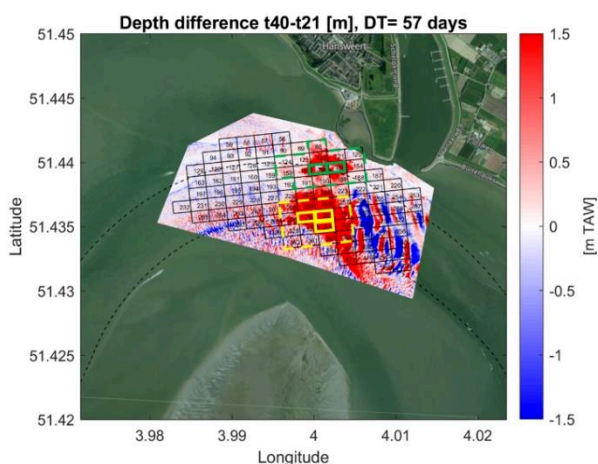

Figure 9 Observed bed level difference [m] in 57 days' time from multibeam-echosounder datasets T40 and T21. Overlaid with black polygons of disposal bins and the navigation channel. Green polygons display the location of the Northen disposal bins (155,156) and the corresponding volume calculation area (dashed line). Yellow polygons display the location of the Southern disposal bins (292, 293 & 326) and the corresponding volume calculation area (dashed line).

C. GAIA adaptations

Multiple adaptations have been implemented in separate FORTRAN files of the GAIA code to perform the simulations, which are treated below.

ZREF: The Van Rijn (1984) equilibrium near-bed concentration formula is given as:

$$C_{eq} = 0.015 d_{50} \frac{\left(\frac{\theta'}{\theta_{cr}}-1\right)^{1.5}}{z_{ref} D_*^{0.3}} \qquad (1)$$

where d_{50} is the median grainsize of the sediment, θ_{cr} is the critical Shields parameter, $\theta' = \mu\theta$ the shear stress due to skin friction, $D*$ is the dimensionless grain diameter of the sediment and z_{ref} is the reference height defined in GAIA as $z_{ref} = 0.5 k_s$ with k_s the total bed roughness. However, following the original paper [14], it is stated that for stability reasons the value of k_s should have a minimal value of $0.01h$, were h denotes the water depth. This formulation was implemented in the 'zref_gaia.f' subroutine and has been applied accordingly in this study. Note that there is no

physical reason for the bed load thickness (and hence z_{ref},) to depend on the water depth. This dependence was added by Van Rijn merely on numerical reasons (namely to avoid the exponential peak in the Rouse profile close to the bed). Therefore, an additional calibration simulation with a constant $z_{ref} = 0.15$ [m] was performed. The results of this simulation are provided in the chapter VI.

POROSITY EFFECTS: A correction factor has been applied to account for the porosity effect on the dilatancy of the sand which influences the erosion. Reference [15] found that in the high velocity range (> 1.5 [m/s]), shearing of sand occurs. Due to this, the porosity increases slightly after which dilatancy yields an inward hydraulic gradient causing a reduction in erosion. Using results from a recent study [16], the following modification to the Van Rijn equilibrium near-bed concentration formula has been made in 'suspension_vanrijn_gaia.f':

$$C_{eq} = 0.015 d_{50} \frac{\left(\frac{\theta'}{\theta_{cr}}-1\right)^{1.5}}{z_{ref} D_*^{0.3}} f_d \qquad (2)$$

Here, f_d stands for the correction factor which is defined as

$$f_d = \begin{cases} 1, & \theta' \le 1 \\ \frac{1}{\theta'}, & \theta' > 1 \end{cases} \qquad (3)$$

The inclusion of the correction factor has a limited impact on the local morphodynamics near the project site of the Put van Hansweert, but tends to effectively stabilize excessive morphological instabilities.

HYBRID-SCHEME AND DISTRIBUTION VERTICAL NODES: In the simulations, the vertical advection and diffusion was calculated using the 'set_dif.f', subroutine, which solves the suspended sediment vertical profile using an implicit scheme and a tridiagonal matrix solver. This subroutine is fast and stable. However, the settling of sediment is calculated using a upwind numerical scheme, which leads to substantial numerical diffusion. Therefore, a hybrid numerical scheme was used [17]. In such a hybrid scheme, an upwind scheme is used for high Peclet numbers (Pe>2, with Pe = uΔz/ν, and u is the velocity, Δz the vertical mesh spacing and the ν diffusivity, when advection is dominant over diffusion), whereas a central scheme is used for low Pe numbers, (i.e. where the physical diffusivity is already high). The results are shown in Figure 10 for a test case in straight uniform open channel flow. The hybrid scheme shows less numerical diffusion than the original scheme. Note that this simulation was performed with a refined mesh near the bottom (twelve vertical nodes).

Initial tests with coarser layer distributions (five & ten sigma layers) revealed very large numerical diffusion, leading to sediment concentrations that are too high, and hence too strong bed erosion. It should be noted that even though the current selected twelve vertical nodes (section II) are the best option so far, since the choice of it is a trade-off between accuracy and computational time & data usage, the selection could be further optimized in future studies.
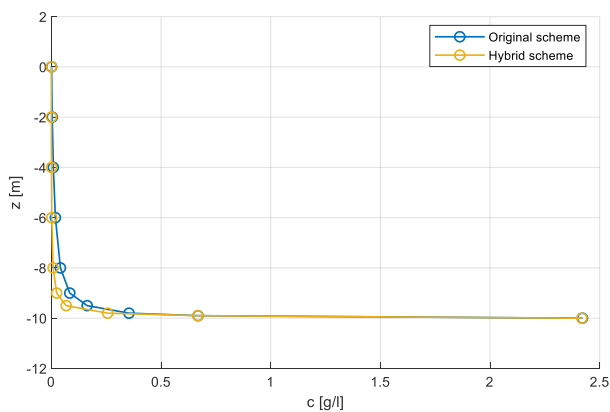
Figure 10 Comparison of original and hybrid advection scheme in straight channel flow simulation.

<u>C-VSM VS HIRANO</u>: Initial tests were performed using the continuous vertical sorting model (C-VSM) [18]. The continuous vertical sorting model is an alternative model for calculating the sorting in the bed, which leads to the formation of stratified sediment layers. This model has the advantage that the stratigraphy of the bed is taken better into account, thus leading to less artificial mixing of sediment in the bed , at the expense of a larger calculation time. In order to use this, the code was changed, such that bed changes due to suspended sediment transport as well as due to bedload were taken into account. However, the results of these tests showed that the C-VSM, in its current form, does not conserve the amount of material, which is essential for the current study, where the amount of fraction1 is used to determine the spreading of the disposed sediment. Some investigations were performed to find the cause of this, and it was found the almost all of the changes in the volume of a certain fraction occurred in the Douglas-Peuker algorithm that is used to simplify the stratigraphy profiles.

VI.   MORPHODYNAMIC CALIBRATION

A qualitative and quantitative validation of the natural morpho-dynamics has been performed by comparing the bed level difference after 46 days from measured multibeam-echosounder datasets, with the simulated bed level difference. In order to determine which of the available equilibrium near-bed concentration equations in GAIA is best suited for the morpho-dynamic modelling tasks of the current study, several simulations with different equations were performed. Results show that there are large differences between the individual equations. Using the Zyserman-Fredsoe formulation, the simulated bed evolutions are extremely high, causing the model to crash within a few simulated days' time. The same holds true when using the Smith and McLean equation (implemented in a user defined Fortran file). Only the Van Rijn (1984) formulation provides realistic bed evolutions, Therefore this equation is selected for further comparison with the observed bed level differences in this section, together with the total load equation of Engelund-Hansen, which is used without advection-diffusion of suspended sediment. This latter applied formula acts as a benchmark equation for river/estuarine morpho-dynamics.

By comparing the measured bed evolution from Figure 11 with the simulated evolutions in Figure 12 (using Van Rijn (1984) equation), it is visible that there is a dynamic area along the inner bend where large-scale bars are migrating upstream. A less dynamic area is visible in the outer bend, which partially corresponds to the region where a stiff non-erodible clay layer is situated. Both measurements and simulation show that there is on average sedimentation on the shoal near the inner bend.
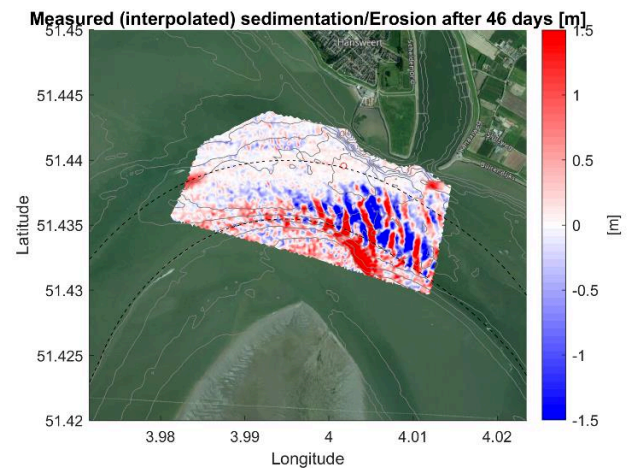

Figure 11 Bed level difference [m] between multibeam-echosounder datasets T20 and T21 (46 days apart), interpolated on top of model mesh.
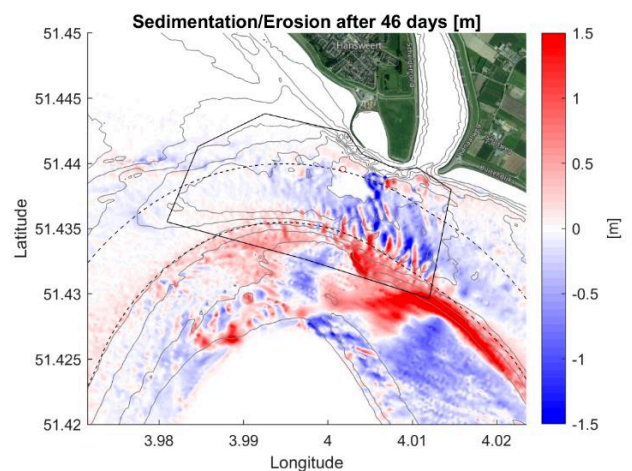

Figure 12 Simulated bed evolution [m] after 46 days with Van Rijn (1984) formula.

The model, using the Van Rijn (1984) equation, has a moderate correlation R = 0.67 [-] with the observed bed evolution and a calculated bias of -0.05 [m]. This shows that simulated bed evolution tends to be slightly more erosive than the measured evolution. Table 5 gives an overview of the statistical parameters for different tested equations. A performed Brier Skill Score (BSS, [19]) analysis of the models with different transport equations, shows that all morpho-dynamic validation simulations perform well. The model using the Van Rijn (1984) equation has a BSS of 0.44 [-]. This implies that the morphodynamical performance of the model has the classification 'Good' (Table 5-3). The BSS of the model with the modified Van Rijn (1984, with constant

z_{ref} = 0.15 [m]) equation has a smaller value (0.34 [-]), but still the classification 'Good'.

The simulation with the Engelund-Hansen total load equation performs even better than the Van Rijn simulations, having the classification 'Excellent'. Though, this total load formula cannot be further used for the analysis of the sediment disposals since three-dimensional sediment concentration fields are applied in the model to simulate the initial spreading of the sediment plume. For this, suspended load transport needs to be calculated by the advection-diffusion equation in TELEMAC-3D.

TABLE 5 OVERVIEW OF STATISTICAL PARAMETERS, CALCULATED FROM THE MEASURED AND MODELLED BED EVOLUTIONS FOR THE DIFFERENT TESTED EQUATIONS.

Equation	Bias [m]	RMSE [m]	Correlation [-]	BSS [-]
Engelund-Hansen	-0.11	0.50	0.75	0.54 (Excellent)
Van Rijn (1984)	-0.05	0.56	0.67	0.44 (Good)
Van Rijn (1984) modified	-0.15	0.60	0.61	0.34 (Good)
Van Rijn (1984) hybrid scheme	-0.12	0.57	0.67	0.41 (Good)

Overall, based on both a qualitative and quantitative validation, the model performs well at the Put van Hansweert and is ready to be used for studying the disposal of sediment.

VII. MORPHODYNAMIC RESULTS

The disposed sediment loss in the first 2.5 months of the realistic reconstructed disposal campaign of autumn 2019 are shown in this section. In this simulation, disposals of both the northern and southern sites are included. From the simulated results, using the Van Rijn (1984) formulation, it can be computed that the loss (i.e., volume outside the northern and southern calculation areas) in the first five weeks of disposal is higher in the model than in the multibeam-echosounder measurements (Figure 13, comparing difference between orange and light-blue lines with difference between red and dark blue lines). To be exact, 40% is lost in the model compared to 36% in the measurements. After this period, the simulated decrease is smaller than the measured decrease. Compared to the estimated measured (linear) loss rate of 2130 [m³/day] in the two months after the last disposal, the modelled loss rate of 1411 [m³/day] is 34% less. It is found that the disposed volume in the model is slightly less than the actual disposed volume, especially in the southern site. This can be explained by volume correction factor that is applied to the CFD sediment plume for every single disposal. Due to a bottom evolution which is more prominent in the southern area, the correction factor is underestimated more than for the northern area. For future iterations, the implementation of the correction factor needs to be improved by taking the effect of the bed evolutions throughout the simulation better into account.

Figure 14 shows that most of the disposed sediment is still confined to its original disposal location after 2.5 months of simulation. Most of the sediment that moves out of the disposal area, tends to migrate in an upstream direction of the main channel. In case of the Northern disposal site, most of the sediment moves along the outer bend, with some sediment moving downstream in the direction of the side channel entry (Middelgat). For the Southern disposal site, most sediment moves along the inner bend. A clear distinction between the sediment disposed in the Northern and Southern bins is visible. This could be explained from a hydrodynamics point of view by the, two individual secondary circulation cells in the bend of the Put van Hansweert (Figure 6). As a result of this, there is a tide averaged flow division in the middle of the channel by which the disposed sediment in the outer bend stays in the outer bend and does not migrate as usual with a helicoidal flow towards the inner bend.
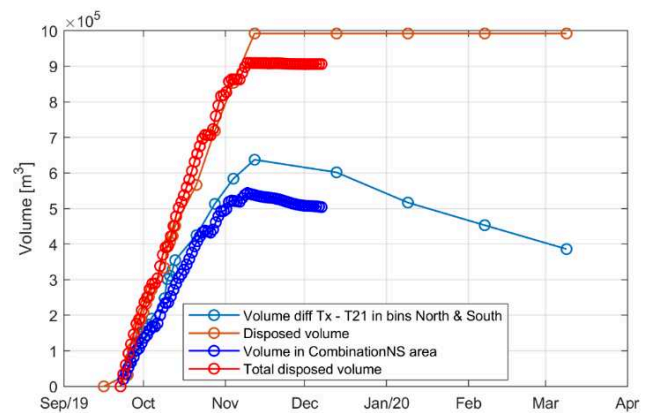

Figure 13 Volume evolution (measured and modelled) of disposed sediment [m³]. Light-blue: observed remaining volume in the Northern & Southern calculation polygons. Orange: total volume of disposed sand. Dark blue: simulated remaining volume of sand in the Northern & Southern calculation polygons. Red: volume of disposed sand in model.
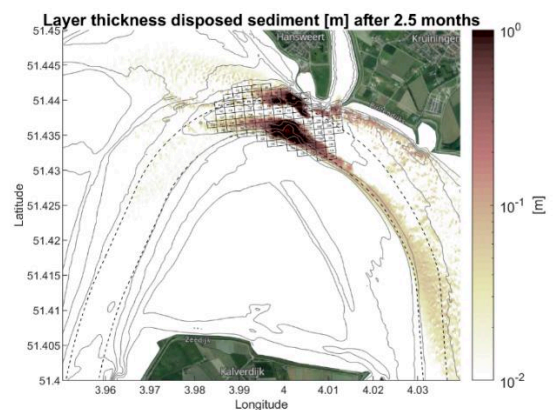

Figure 14 Layer thickness of disposed sediment (northern & southern area) after 2.5 months. Layer thickness scale is saturated.

In order to provide an estimation of the migration directions of the disposed sediment, the region surrounding the Put van Hansweert is divided into ten separate calculation polygons in which the volumes of disposed sediment are calculated. Figure 15 shows that the largest amount of sediment, aside from the disposal polygons, is found upstream in polygon 8 (8.1%) and on the outer bend of the

Put van Hansweert in polygon 10 (6.9%). Of the sediment found in the relatively large polygon 10, the layer thickness map (Figure 14) indicates that the largest amount is found at the outer bend of the Put van Hansweert and at the edge of the main navigation channel. Of the total disposed 0.9 [M m^3] sediment, only 2.3% is found back downstream in the Middelgat side channel (polygon 1).
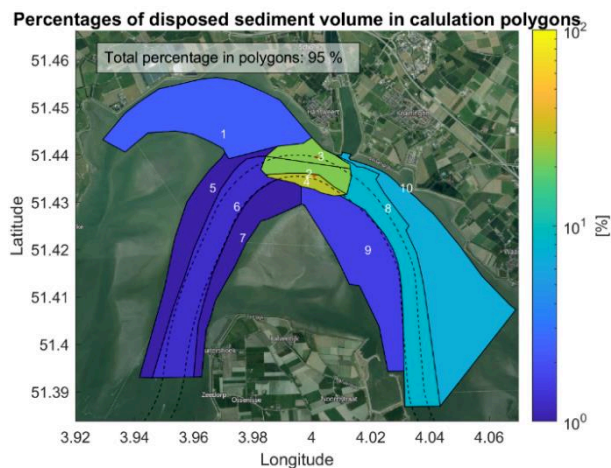

Figure 15 Percentage of disposed volume found in polygons after 2.5 months.

VIII.   CONCLUSIONS

In this study, numerical simulations were performed with the morpho-dynamic TELEMAC-3D Scheldt model to investigate the behaviour of disposed non-cohesive sediment in the Put van Hansweert. More specifically, the model has been deployed to reproduce the experimental disposal campaign of autumn 2019 at the Put van Hansweert.

From the hydrodynamical validation process, it has become evident that the salinity plays a crucial role in the generation of the local (secondary) cross-currents at the Put van Hansweert. Without the effect of salinity, the usual helicoidal flow is observed. However, when salinity is included in the model, the generation of two circulation cells is observed which can act as a barrier for sediment to move from the outer bend towards the inner bend.

A scenario simulation has been constructed which reproduces the experimental disposal campaign of autumn 2019 at the Put van Hansweert in a long-term 2.5-month simulation. Results show that the modelled sediment losses are close to the measured values of losses. The majority of the in total 0.9 [M m^3] disposed sediment in the model is still confined to its original disposal location after 2.5 months of simulation. Most of the sediment that moves out of the disposal area tends to migrate in an upstream direction. In case of sediment disposals in the Northern disposal area, the main migration route is along the outer bend of the channel with limited potential transport to the side channels. In case of the Southern disposed area, the main migration is along the inner bend of the main channel.

By performing multiple sensitivity analyses, it is found that the stability of the disposed sediment is mostly affected by the choice of the equilibrium near-bed concentration formula and by the choice of the number and distribution of vertical nodes in TELEMAC-3D. Numerical schemes for the vertical sediment transport in TELEMAC show a substantial amount of numerical diffusion. Therefore, a new hybrid upwind/central advection schemes was used, which shows less numerical diffusion. Nevertheless, the morphological results are not very sensitive to the choice of the scheme, provided that proper calibration of the model is performed.

REFERENCES

[1] Huisman B.J.A., Huismans Y. & Vroom J. (2021). Effecten van storten in diepe putten van de Westerschelde. Synthese van proefstortingen en modelanalyses. Deltares rapport 1210301-015-ZKS-0012.

[2] IMDC (2021). Analyserapport proefstortcampagne Inloop van Ossenisse en Put van Hansweert. I/RA/11498/20.063/API/

[3] IMDC & Deltares (2018). Detailanalyse Morfologische respons op de proefstortingen in de put van Hansweert. I/RA/12161/18.013/THL/.

[4] Plancke Y., Bastiaensen E. & Mostaert, F. F. (2020a). Proefstortingen Westerschelde Deelrapport 2 – Analyse beun- en boxcorerstalen bij de uitvoering van de stortproef 2019 in de diepe put van Hansweert. Versie 4.0. WL Rapporten, 19_079_2.

[5] Vanlede J., Smolders S., Maximova T. & Teles M.J. (2015). The unstructured Scaldis model: A new 3D high resolution model for hydrodynamics and sediment transport in the tidal Scheldt. Proc Scheldt Estuary Phys. Integr. Manag. Sess. 36th IAHR World Congr.

[6] Chu K., Breugem A., Wolf T. & Decrop B. (2020). Improvement of a Continental Shelf Model of the North Sea. TELEMAC User Conference, Antwerp, Belgium.

[7] Egbert G.D. & Ray R.D. (2001). Estimates of M2 tidal energy dissipation from TOPEX/Poseidon altimeter data. J. Geophys. Res. Oceans, 106(C10), 22475–22502.

[8] Sutherland J. & Soulsby R. (2003). Use of model performance statistics in modelling coastal morphodynamics. Proc. Int. Conf. Coast. Sediments.

[9] Huismans Y., van der Vegt H., Huisman B. & Colina Alonso A. (2021). Westerschelde: storten in diepe putten. Technische rapportage: mesoschaal morfologische ontwikkelingen rond de Put van Hansweert. Deltares rapport 1210301-015-ZKS-0011.

[10] McLaren (1994). sediment transport in the westerschelde between baarland and rupelmonde.

[11] S.H.L.L. Gruijters, Schokker J. & Veldkamp J.G. (2004). Kartering Moeilijk Erodeerbare Lagen in Het Schelde Estuarium, Rapport nr 03-213-B1208.

[12] Van der Vegt H., Mastbergen D. & Van der Werf J. (2019). Moeilijk-erodeerbare lagen in de Westerschelde. Onzekerheden en gevolgen voor morfodynamiek.

[13] IMDC (2020b). VNSC Project Diepe Delen - Report on CFD calculations of disposal plumes. I/RA/12161/20.005/BDC/FKY

[14] Van Rijn L.C. (1984). Sediment transport, Part II: Suspended load transport. J. Hydraul. Eng., 110(11), 1613–1641.

[15] van Rhee C. (2010). Sediment entrainment at high flow velocity. J. Hydraul. Eng., 136(9).

[16] Rijn L.C.V., van Rhee C. & Bisschop R. (2019). Modified Sediment Pick-Up Function. J. Hydraul. Eng., 145(1).

[17] Patankar, S. V. (1980). Numerical heat transfer and fluid flow(Book). Washington, DC, Hemisphere Publishing Corp., 1980. 210 p.

[18] Merkel, U. (2017). C-VSM-II: Large scale and long time simulations with Sisyphe's continuous vertical grain sorting model. In Proceedings of the XXIVth TELEMAC-MASCARET User Conference, 17 to 20 October 2017, Graz University of Technology, Austria (pp. 131-138).

[19] Sutherland J., Peet A. & Soulsby R. (2004a). Evaluating the performance of morphological models. *Coast. Eng.*, <u>51</u>, 917–939.